A functional equation for the specular reflection of rays

A. Le Bot[a)]
Laboratoire de Tribologie et Dynamique des Systèmes, École Centrale de Lyon, 36, Avenue Guy de Collongues 69134 BP163 Ecully, France

(Received 2 October 2000; revised 29 June 2002; accepted 10 July 2002)

This paper aims to generalize the ''radiosity method'' when applied to specular reflection. Within the field of thermics, the radiosity method is also called the ''standard procedure.'' The integral equation for incident energy, which is usually derived for diffuse reflection, is replaced by a more appropriate functional equation. The latter is used to solve some specific problems and it is shown that all the classical features of specular reflection, for example, the existence of image sources, are embodied within this equation. This equation can be solved with the ray-tracing technique, despite the implemented mathematics being quite different. Several interesting features of the energy field are presented. © *2002 Acoustical Society of America.* [DOI: 10.1121/1.1504854]

PACS numbers: 43.20.Dk, 43.20.EI [ANN]

LIST OF SYMBOLS

ν	position parameter at the boundary
θ	emission angle
φ	incidence angle
$\mathbf{r}$	receiver point
$\mathbf{s}$	source point
$\mathbf{p}$	point at the boundary
W	energy density
$\mathbf{I}$	intensity vector
G	direct field for energy density
$\mathbf{H}$	direct field for intensity
ω	circular frequency
c	speed of sound
m	attenuation factor

I. INTRODUCTION

The fact that waves propagate like rays is undoubtedly the oldest idea in wave motion. Many ideas on this topic have already been developed in depth. Rays have lost their fundamental status and are now regarded as high-frequency approximation of waves. The concept of ray is only valid for short wavelengths. However, rays are still widely encountered in modern science for several reasons.

First, solving governing wave equations is practical only for low frequencies due to computational limits of the finite-element method. At higher frequencies, ray methods are used and are often the only feasible solution. For instance, for room acoustics, the finite-element method is rarely applied. The majority of the audio range may be investigated using the ray-tracing technique[1] or other simple formulas based on the statistical properties of rays.[2]

Second, ray theories enable the ray paths and magnitudes to be determined separately. In some fields, only the paths are of interest, for instance the image formation study used for optical instrument design. Geometrical optics is a direct means of gaining access to targeted information without solving sophisticated equations.

Finally, beyond a mere approximation, ray theories may be regarded as an original view of wave motion whose spirit is quite different from the classical one. Many vibrational phenomena can be translated into ray terms, resulting in a particularly clear and intuitive representation.

For several years, a method based on energy considerations has been investigated in room acoustics.[3–5] This method leads to an integral equation where the unknown is the incident energy at the boundary. The equation has been applied to the calculation of time reverberation for rooms with nondiffuse noise. This method, sometimes called the ''radiosity method,'' [6] seems to stem from the ''standard procedure'' in thermics.[7] The problem of radiative heat exchange between n diffusely reflecting surfaces is reduced to a set of n-linear algebraic equations, coefficients of which are usually called view factors or angle factors. In Refs. 8 and 9, this method has been extended to structural acoustics. The radiosity method is actually a true ray method,[10] although its numerical implementation is quite different from that of classical ray-tracing algorithms. However, the radiosity method assumes ideally diffuse reflection at walls, whereas the ray-tracing technique is not limited to a particular law of reflection. A generalization of the radiosity method for partially diffuse reflection has been proposed in Ref. 11, where both the integral equation and the image-source technique are jointly employed. The effect of specular reflection leads to additional sources distributed behind the boundary, whereas the sources created by the diffuse reflection are localized at the boundary. This paper aims to adapt the radiosity method to *perfectly specular reflection* with some *sources localized on the boundary*. The integral equation is replaced by a more appropriate functional equation. The modified equation remains a ray method, and a large part of the paper is devoted to verifying that solutions of this equation match the classical properties of rays.

The outline of the present paper is as follows. In Sec. III, the vibration field is separated into elementary waves. These

a)Electronic mail: alain.le-bot@ec-lyon.fr

waves are assumed to be totally uncorrelated and consequently their energies are added to obtain the complete field. Some basic properties are also reviewed. In Secs. IV and V, a systematic application of the energy balance gives a set of equations for these energy variables. Section VI shows how the classical image-source method may be applied to solve the energy equations. A second example is studied in Sec. VII. Section VIII proposes an interpretation of in terms of rays. Finally, this theory is applied to a circular domain in Sec. IX.

II. MOTIVATION FOR THE STUDY

When using the radiosity method, it is assumed that the rays are ideally diffusely reflected. The cosine Lambert's law can be applied to fictitious sources of magnitude σ, which are distributed over the boundary Γ. The reflected energy at any point $\mathbf{r}$ inside the domain Ω is written

$$\int_{\Gamma} \sigma(\nu)\cos\theta \frac{d\nu}{r} \tag{1}$$

(two-dimensional case), where ν is the curvilinear abscissa of the boundary Γ, θ the emission angle, and $r=|\mathbf{r}-\mathbf{p}|$ the distance between the receiver point $\mathbf{r}$ and the fictitious source located at $\mathbf{p}$ of abscissa ν. The reflected energy is proportional to $1/r$.

The purpose of this paper is to extend the radiosity method to the case of pure specular reflection. However, it is expected that the reflected energy may still result from some fictitious sources distributed over the boundary as in Eq. (1). It is well-known that a source in front of a plane surface gives rise to a single image source, say $\mathbf{s}$. The reflected energy is thus $1/R$, where $R=|\mathbf{s}-\mathbf{r}|$ is the source–receiver distance. The question now arising is whether the reflected field $1/R$ can result from equivalent sources distributed over the boundary

$$\int_{\Gamma} \sigma(\nu,\theta)\frac{d\nu}{r} \stackrel{?}{=} \frac{1}{R}, \tag{2}$$

for a well-chosen function σ which is no longer restricted to follow Lambert's law. The answer is yes. To check this assertion, consider

$$\sigma(\nu,\theta)=\delta(\theta-\varphi)\cos\theta/l, \tag{3}$$

where $l=|\mathbf{s}-\mathbf{p}|$ is the distance between the image-source $\mathbf{s}$ and the fictitious source $\mathbf{p}$ of abscissa ν, and φ is the incidence angle [Fig. 1(a)]. With a change of variable $\nu\rightarrow\psi=\varphi-\theta$

$$\int_{-\infty}^{\infty}\delta(\theta-\varphi)\frac{\cos\theta}{l}\frac{d\nu}{r}=\int\delta(\psi)\frac{\cos\theta}{l}\frac{1}{r}\frac{d\nu}{d\psi}d\psi = \frac{\cos\theta_0}{l_0\times r_0}\Big/\left.\frac{d\psi}{d\nu}\right|_{\nu=\nu_0}, \tag{4}$$

where ν_0 is the position where the emission angle θ_0 is equal to the incidence angle φ_0, i.e., $\psi=0$. l_0, r_0 are the corresponding source–boundary and boundary–receiver distances [Fig. 1(a)]. An infinitesimal displacement $d\nu$ can be expressed as $d\nu=-rd\theta/\cos\theta$ [Fig. 1(b)]. Likewise, variation in $d\varphi$ results in $d\nu=ld\varphi/\cos\varphi$, and thus

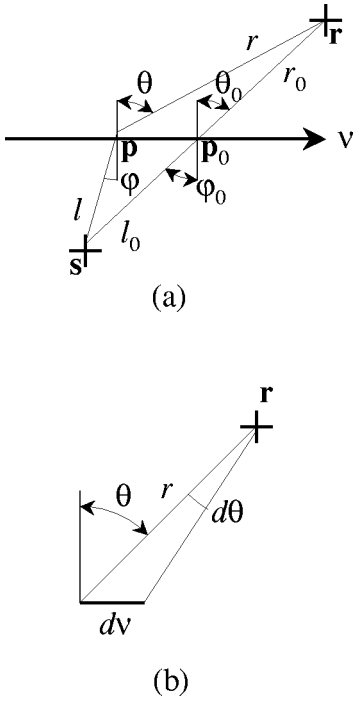

FIG. 1. Description of an image-source $\mathbf{s}$, which is behind the boundary, in terms of the fictitious sources located on the boundary.

$$\frac{d\psi}{d\nu}=\frac{d\varphi}{d\nu}-\frac{d\theta}{d\nu}=\frac{\cos\varphi}{l}+\frac{\cos\theta}{r}. \tag{5}$$

By substituting Eq. (5) into Eq. (4), the reflected energy is found to be

$$\frac{\cos\theta_0}{l_0\times r_0}\Big/\left(\frac{\cos\varphi_0}{l_0}+\frac{\cos\theta_0}{r_0}\right)=\frac{1}{l_0+r_0}=\frac{1}{R}, \tag{6}$$

since $\theta_0=\varphi_0$ and $R=l_0+r_0$. The expected result is thus obtained.

The plan is now to exploit this result and extend it for a general representation of reflected energy. Indeed, the question is how to determine the fictitious source distribution σ. It is shown in Sec. IV that the distribution σ is determined by a functional equation.

III. ENERGY REPRESENTATION OF WAVES

In the context of *linear acoustics with homogeneous and isotropic fluid*, two energy fields are referred to: the energy density $W=\rho|\mathbf{v}|^2/2+p^2/2\rho c^2$, where p is the acoustical pressure, $\mathbf{v}$ the velocity, ρ the volumic mass of fluid, and c the speed of sound, and the energy flow or intensity $\mathbf{I}=p\mathbf{v}$. The circular frequency is denoted as ω and the speed of the flow of energy is denoted as c. Various kinds of damping mechanisms are possible. The atmospheric absorption originates from several phenomena: dynamical viscosity of fluid, molecular absorption, etc. A local relationship is adopted between the power density which is dissipated p_{diss} and the energy density W, $p_{\text{diss}}=mcW$, where m is the attenuation factor. As the factor m is ω-dependent, this expression does not hold in the time domain. However, it remains an inter-

esting approximation for some transient problems which involve wave packets such as time reverberation in acoustics or structural acoustics, time arrival of rays in ultrasonic propagation, and so on. A simple proportional relationship holds between the energy flow and the energy density[12] of traveling waves, $I=cW$, where I is the magnitude of the energy flow vector $\mathbf{I}$. This relationship cannot be verified within the neighborhood of the excitation point, but it is applied under the assumption that *evanescent wave and the near field are neglected*.

Now, consider the direct field of a source $\mathbf{s}$ of unit power. In steady-state condition, $G(\mathbf{s},\mathbf{r})$ denotes the energy density at any point $\mathbf{r}$ and $\mathbf{H}(\mathbf{s},\mathbf{r})$ denotes the intensity. In the case of a transient source, the notation $G(\mathbf{s},\tau;\mathbf{r},t)$ and $\mathbf{H}(\mathbf{s},\tau;\mathbf{r},t)$ is used for the direct fields generated by an impulse excitation at $\mathbf{s}$ at time τ. The energy balance is then

$$\mathrm{div}_{\mathbf{r}}\cdot\mathbf{H}+mcG+\frac{\partial G}{\partial t}=\delta_{\mathbf{s},\tau}, \tag{7}$$

where the first term in the left-hand side is the net outgoing power per unit volume and the second term is the power density which is dissipated p_{diss}. The fields G and $\mathbf{H}$ depend only on the distance $s=|\mathbf{r}-\mathbf{s}|$. With the condition $H=cG$, the fields G and $\mathbf{H}$ can readily be found[8,9]

$$G(\mathbf{s},\mathbf{r})=\frac{1}{\gamma_0 c}\frac{e^{-ms}}{s^{n-1}}, \tag{8}$$

$$G(\mathbf{s},\tau;\mathbf{r},t)=G(\mathbf{s},\mathbf{r})\,\delta(t-\tau-s/c), \tag{9}$$

where $\gamma_0=2\pi$ or 4π depending on the dimension n. Furthermore, $\mathbf{H}=cG\mathbf{u_{sr}}$, where $\mathbf{u_{sr}}=(\mathbf{r}-\mathbf{s})/|\mathbf{r}-\mathbf{s}|$ is the unit vector from $\mathbf{s}$ to $\mathbf{r}$.

Actual sources rarely have a uniform output. For the nonuniform case, it is convenient to introduce the directional emissive power density $\rho(\mathbf{s},\mathbf{u},\tau)$, which gives the power injected along the direction $\mathbf{u}$ at time τ and at point $\mathbf{s}$. Directionality is not usually time dependent and thus $\rho(\mathbf{s},\mathbf{u},\tau)=f_{\mathbf{s}}(\mathbf{u})\rho(\tau)$, where $f_{\mathbf{s}}(\mathbf{u})$ is the directional function of the source $\mathbf{s}$. The injected power density p_{inj} is obtained by integrating the flux of $\rho\mathbf{H}$ over an infinitesimal sphere which surrounds the point $\mathbf{s}$

$$p_{\mathrm{inj}}(\mathbf{s},\tau)=\frac{1}{\gamma_0}\int_{S_{n-1}}\rho(\mathbf{s},\mathbf{u},\tau)\,dS_{\mathbf{u}}, \tag{10}$$

where dS is the surface measure on the unit sphere S_{n-1}. For an isotropic source, this relationship reduces to $p_{\mathrm{inj}}=\rho$.

Let us turn to the case where several sources simultaneously act in a bounded or unbounded smooth domain Ω with boundary Γ. To ensure a meaning for all subsequent integrals, it is assumed that an outward normal exists almost everywhere. It is also assumed that *all sources are uncorrelated* in order that linear superposition principle may be applied to energy fields. This approximation leads to the neglect of all interference effects and, as a consequence, modes cannot be predicted. The fields W and $\mathbf{I}$ result from the superposition of direct fields which emerge from primary sources ρ and diffracted fields which emerge from secondary sources σ distributed on the boundary Γ. For any $\mathbf{r}\in\Omega$

$$W(\mathbf{r},t)=\int_{\Omega}\rho(\mathbf{s},\mathbf{u_{sr}},t-s/c)G(\mathbf{s},\mathbf{r})\,d\Omega_{\mathbf{s}}+\int_{\Gamma}\sigma(\mathbf{p},\mathbf{u_{pr}},t-r/c)G(\mathbf{p},\mathbf{r})\,d\Gamma_{\mathbf{p}}, \tag{11}$$

$$\mathbf{I}(\mathbf{r},t)=\int_{\Omega}\rho(\mathbf{s},\mathbf{u_{sr}},t-s/c)\mathbf{H}(\mathbf{s},\mathbf{r})\,d\Omega_{\mathbf{s}}+\int_{\Gamma}\sigma(\mathbf{p},\mathbf{u_{pr}},t-r/c)\mathbf{H}(\mathbf{p},\mathbf{r})\,d\Gamma_{\mathbf{p}}, \tag{12}$$

where $s=|\mathbf{r}-\mathbf{s}|$ and $r=|\mathbf{r}-\mathbf{p}|$. $d\Omega$ is the Lebesgue measure in Ω, whereas $d\Gamma$ is the surface measure on Γ. The main difference between Eqs. (11), (12), and the corresponding equations for the radiosity method appears in the nature of the variable σ, which here depends on the direction $\mathbf{u_{pr}}$. The radiosity method is thus embodied in Eqs. (11) and (12) by adopting Lambert's law $\sigma(\mathbf{p},\mathbf{u},\tau)=\sigma(\mathbf{p},\tau)\cos\theta$, where θ is the emission angle between the outward normal of the boundary $\mathbf{n}$ and $\mathbf{u}$. The focus of this text is to show that by adopting well-chosen distributions σ, the diffracted field can become a plane wave or a cylindrical wave, which emanates from a unique image source. This result is surprising since the function G in Eq. (11) is a cylindrical wave.

The local power balance for the fields W and $\mathbf{I}$ is

$$\mathrm{div}.\mathbf{I}+mcW+\frac{\partial W}{\partial t}=p_{\mathrm{inj}}, \tag{13}$$

where p_{inj} has been given in Eq. (10). This can be checked by a direct substitution of Eqs. (11) and (12) on the left-hand side and by using Eq. (7) (Appendix A). The global power balance for the whole system Ω is obtained by integrating Eq. (13) over Ω. It yields

$$P_{\mathrm{out}}+mcW_{\Omega}+\frac{\partial W_{\Omega}}{\partial t}=P_{\mathrm{inj}}, \tag{14}$$

where $W_{\Omega}=\int_{\Omega}W\,d\Omega$ denotes the energy of the domain Ω. $P_{\mathrm{out}}=\int_{\Gamma}\mathbf{I}.\mathbf{n}\,d\Gamma$ is the outward energy flow. $P_{\mathrm{inj}}=\int_{\Omega}p_{\mathrm{inj}}\,d\Omega$ is the total power supplied by primary sources. This equality shows that for isolated systems ($P_{\mathrm{out}}=0$) in a steady-state condition with finite injected power ($P_{\mathrm{inj}}<\infty$), the total energy W_{Ω} is finite, i.e., the integral $\int_{\Omega}W\,d\Omega$ must converge. This result is not trivial for two reasons. First, the field W is singular in general. Isolated source points or focus points in certain situations may lead to singularities of W. Second, the domain Ω may be bounded or unbounded. In the latter case, the decrease of W in the far field must be sufficiently strong to ensure the convergence.

The relationships (11) and (12) give the fields W and $\mathbf{I}$ at any point within the domain Ω. But, similar relationships for the boundary Γ have not yet been sought although they are of interest from a theoretical point of view. The fields W and $\mathbf{I}$ for a regular point $\mathbf{p}\in\Gamma$ are

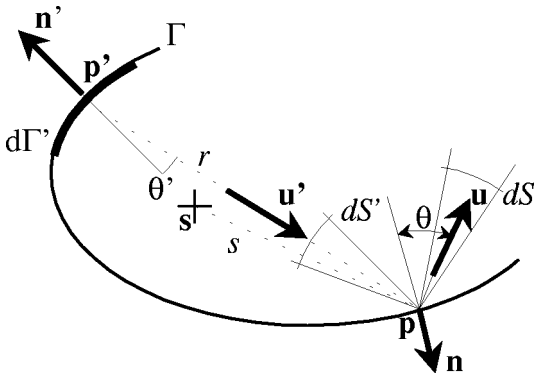

FIG. 2. Energy balance for **p** at the boundary; incident power stems from both actual sources **s**, which are located within the incident cone, and diffraction sources $\mathbf{p}'$, which are located on the part $d\Gamma'$ of the boundary.

$$W(\mathbf{p},t)=\int_{\Omega}\rho(\mathbf{s},\mathbf{u_{sp}},t-s/c)G(\mathbf{s},\mathbf{p})d\Omega_{\mathbf{s}}+\int_{\Gamma}^{*}\sigma(\mathbf{q},\mathbf{u_{qp}},t-r/c)G(\mathbf{q},\mathbf{p})d\Gamma_{\mathbf{q}}+\int_{HS}\frac{\sigma(\mathbf{p},\mathbf{u},t)}{\gamma_0 c\cos\theta}dS_{\mathbf{u}}, \tag{15}$$

$$\mathbf{I}(\mathbf{p},t)=\int_{\Omega}\rho(\mathbf{s},\mathbf{u_{sp}},t-s/c)\mathbf{H}(\mathbf{s},\mathbf{p})d\Omega_{\mathbf{s}}+\int_{\Gamma}^{*}\sigma(\mathbf{q},\mathbf{u_{qp}},t-r/c)\mathbf{H}(\mathbf{q},\mathbf{p})d\Gamma_{\mathbf{q}}+\int_{HS}\frac{\sigma(\mathbf{p},\mathbf{u},t)}{\gamma_0\cos\theta}\mathbf{u}\,dS_{\mathbf{u}}. \tag{16}$$

The asterisk designates the principal value of Cauchy. *HS* is the unit hemisphere of inward unit vectors, which is centered at **p**. Equations (15) and (16) are proved in Appendix A.

IV. SPECULAR REFLECTION AT BOUNDARY

This section is concerned with the derivation of an appropriate equation for the unknown σ on the basis of *specular reflection*. This equation is derived by applying the power balance at the boundary at any regular point $\mathbf{p}\in\Gamma$. Consider a solid angle dS along an emission direction **u**. The incident solid angle is dS' along $\mathbf{u}'$. Specularity implies that $\mathbf{u}'$, **u**, and **n** are coplanar, $\cos\theta=|\mathbf{u}\cdot\mathbf{n}|=|\mathbf{u}'\cdot\mathbf{n}|$ and $dS'=dS$. Let $\mathbf{p}'$ designate the point at the boundary from which the incident direction $\mathbf{u}'$ originates (Fig. 2). This point may or may not exist. It may or may not be unique. For simplicity, the ensuing calculation is performed for the case in which if $\mathbf{p}'$ exists, it is unique. Other cases are discussed below.

The incident power at **p** arising from primary sources **s** situated within the incident cone is denoted $\mathcal{P}_{\mathrm{dir}}$. The incident power due to secondary sources which are located within the region $d\Gamma'$ of the boundary which intersects the incident cone is denoted $\mathcal{P}_{\mathrm{dif}}$. The infinitesimal power emitted is denoted $\mathcal{P}_{\mathrm{emit}}$. Introducing an absorption coefficient α defined as the ratio of absorbed power over incident power, the power balance is

$$\mathcal{P}_{\mathrm{emit}}=[1-\alpha][\mathcal{P}_{\mathrm{dir}}+\mathcal{P}_{\mathrm{dif}}]. \tag{17}$$

The emitted power $\mathcal{P}_{\mathrm{emit}}$ is the flux of the energy flow vector from the source **p** of magnitude $\sigma(\mathbf{p},\mathbf{u},t)$ through the region of the sphere with a small radius ϵ which intersects the reflected cone dS. The area of this surface is $\epsilon^{n-1}\,dS$. Then

$$\mathcal{P}_{\mathrm{emit}}=\lim_{\epsilon\to 0}\left(\sigma(\mathbf{p},\mathbf{u},t-\epsilon/c)\frac{e^{-m\epsilon}}{\gamma_0\epsilon^{n-1}}\epsilon^{n-1}\,dS\right)=\sigma(\mathbf{p},\mathbf{u},t)\frac{dS}{\gamma_0}. \tag{18}$$

The incident power $\mathcal{P}_{\mathrm{dir}}$ stemming from the primary sources that are located inside the incident cone dS' is

$$\mathcal{P}_{\mathrm{dir}}=\int_{\mathbf{p}'\mathbf{p}}\rho(\mathbf{s},\mathbf{u}',t-s/c)\mathbf{H}(\mathbf{s},\mathbf{p})\cdot\mathbf{n}s^{n-1}\,ds\,dS'=\frac{1}{\gamma_0}\int_{\mathbf{p}'\mathbf{p}}\rho(\mathbf{s},\mathbf{u}',t-s/c)e^{-ms}\,ds\cos\theta\,dS', \tag{19}$$

where $s=|\mathbf{p}-\mathbf{s}|$. $s^{n-1}ds\,dS'$ is the infinitesimal volume in spherical coordinates. The integral is performed over the segment $\mathbf{p}'\mathbf{p}$. The incident power $\mathcal{P}_{\mathrm{dif}}$ stemming from secondary sources located on $d\Gamma'$ is

$$\mathcal{P}_{\mathrm{dif}}=\sigma(\mathbf{p}',\mathbf{u}',t')\mathbf{H}(\mathbf{p}',\mathbf{p})\cdot\mathbf{n}\,d\Gamma', \tag{20}$$

where $t'=t-r/c$ and $r=|\mathbf{p}-\mathbf{p}'|$. The infinitesimal surface $d\Gamma'$ is related to the solid angle dS' by $d\Gamma'=r^{n-1}dS'/\cos\theta'$, where θ' is the emission angle at $\mathbf{p}'$

$$\mathcal{P}_{\mathrm{dif}}=\frac{1}{\gamma_0}\sigma(\mathbf{p}',\mathbf{u}',t')e^{-mr}\frac{\cos\theta}{\cos\theta'}dS'. \tag{21}$$

By substituting Eqs. (18), (19), (21) into the power balance (17), the equation for σ is obtained for any regular point $\mathbf{p}\in\Gamma$

$$\frac{\sigma(\mathbf{p},\mathbf{u},t)}{\cos\theta}=(1-\alpha)\left[\frac{\sigma(\mathbf{p}',\mathbf{u}',t')}{\cos\theta'}e^{-mr}+\int_{\mathbf{p}'\mathbf{p}}\rho(\mathbf{s},\mathbf{u}',t-s/c)e^{-ms}\,ds\right]. \tag{22}$$

Equation (22) relates the value of σ at $(\mathbf{p},\mathbf{u},t)$ to the value of σ at $(\mathbf{p}',\mathbf{u}',t')$. It is thus a functional equation of the unknown σ.

If the point $\mathbf{p}'$ does not exist, the corresponding incident power $\mathcal{P}_{\mathrm{dif}}$ must be removed from the previous calculation. The first term of the right-hand side of Eq. (22) vanishes and Eq. (22) yields the direct solution of σ. In the case where $\mathbf{p}'$ is not unique, the contributions of all these points must be accounted for the calculation of $\mathcal{P}_{\mathrm{dif}}$. The complexity of the resulting expression depends upon whether there are a finite, countable infinite or uncountable infinite number of points. This case is not considered.

V. REFRACTION AT INTERFACE

The subscript $i=1,2$ is now introduced to denote both domains separated by an interface. Consider a point $\mathbf{p}\in\Gamma_1\cap\Gamma_2$ located on the interface. $\mathbf{n}_i$ $i=1,2$ denotes the outward unit normal at **p** ($\mathbf{n}_1=-\mathbf{n}_2$). Two diffraction sources

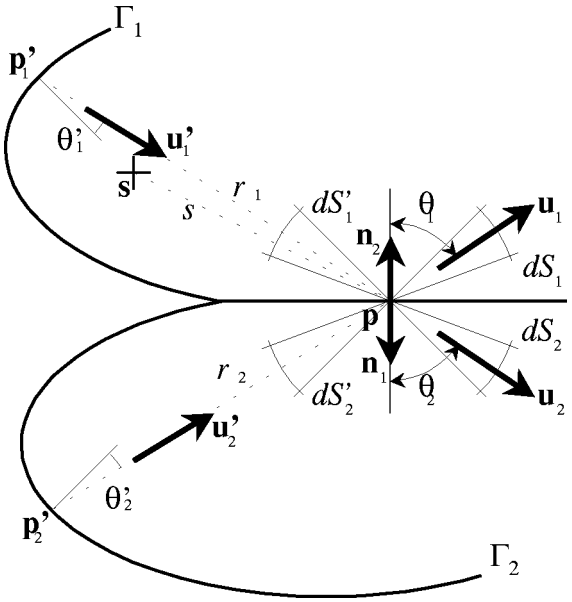

FIG. 3. Energy balance for $\mathbf{p}$ at the interface; power emitted toward $\mathbf{u}_1$ stems from the actual and the diffraction sources within Ω_1 and Ω_2.

σ_1 and σ_2 are present, one on each side of the interface. The incident power at $\mathbf{p}$ arising from the domain Ω_1 for instance, is partially reflected back towards Ω_1 and is also partially transmitted into Ω_2. If $\mathbf{u}_1'$ is the incident unit vector, $\mathbf{u}_1$ the reflected direction with emission angle θ_1, and $\mathbf{u}_2$ the refracted direction with emission angle θ_2, then the vectors $\mathbf{n}_1$, $\mathbf{n}_2$, $\mathbf{u}_1'$, $\mathbf{u}_1$, and $\mathbf{u}_2$ are coplanar and Snell's law states that $\sin\theta_1/c_1'=\sin\theta_2/c_2'$ where c_i' is the phase velocity in the medium i. The notations are summarized in Fig. 3.

The efficiency τ_{ij} is defined as the ratio of incident power coming from Ω_i to the power re-emitted towards Ω_j. This efficiency depends on the position $\mathbf{p}$ and the incident direction. When using a ray model, reflection and refraction phenomena follow the *principle of locality*. This allows the calculation of closed-form relationships. Deriving these efficiencies is a classical problem which is solved for many wave configuration in the literature.[13,14] It should be added that when the ''plane wave–plane surface'' approximation is applied to a general wave which impinges upon a curvilinear surface, the order of approximation is zero.[15] The efficiencies τ_{ij} must verify several constraints. The efficiencies are nonnegative factors less than unity

$$0\leqslant\tau_{ij}\leqslant 1. \tag{23}$$

If the interface is nondissipative, conservation of energy ensures that $\Sigma_j\tau_{ij}=1$. When absorption occurs, this sum is less than 1, $\Sigma_j\tau_{ij}<1$. By introducing the absorption coefficient α of the interface[16]

$$\sum_j \tau_{ij}+\alpha=1. \tag{24}$$

According to the *reciprocity principle*[17]

$$\tau_{ij}=\tau_{ji}. \tag{25}$$

This equality is only true along directions which are related to each other through Snell's law. However, the reciprocity principle does not hold for all systems. Counter examples do exist.[18]

Let us turn to the derivation of the functional equations for the secondary sources σ_1 and σ_2. The power emitted towards Ω_1, for instance, is the reflected part of the incident power stemming from the sources in Ω_1 plus the refracted part of the incident power stemming from the sources in Ω_2 (Fig. 3)

$$P_{1,\mathrm{emit}}=\tau_{11}[\mathcal{P}_{1,\mathrm{dir}}+\mathcal{P}_{1,\mathrm{dif}}]+\tau_{21}[\mathcal{P}_{2,\mathrm{dir}}+\mathcal{P}_{2,\mathrm{dif}}], \tag{26}$$

$$P_{2,\mathrm{emit}}=\tau_{12}[\mathcal{P}_{1,\mathrm{dir}}+\mathcal{P}_{1,\mathrm{dif}}]+\tau_{22}[\mathcal{P}_{2,\mathrm{dir}}+\mathcal{P}_{2,\mathrm{dif}}]. \tag{27}$$

The emitted powers were calculated in Eq. (18)

$$\mathcal{P}_{i,\mathrm{emit}}=\sigma_i(\mathbf{p},\mathbf{u}_i,t)\frac{dS_i}{\gamma_0}. \tag{28}$$

Similarly, Eqs. (19) and (21) are still valid

$$\mathcal{P}_{i,\mathrm{dir}}=\frac{1}{\gamma_0}\int_{\mathbf{p}_i'\mathbf{p}}\rho_i(\mathbf{s},\mathbf{u}_i',t-s/c_i)e^{-m_i s}ds\cos\theta_i\,dS_i', \tag{29}$$

for the incident power from the direct field and

$$\mathcal{P}_{i,\mathrm{dif}}=\frac{1}{\gamma_0}\sigma_i(\mathbf{p}_i',\mathbf{u}_i',t_i')e^{-m_i r_i}\frac{\cos\theta_i}{\cos\theta_i'}dS_i', \tag{30}$$

for the incident power from the diffracted field where $t_i'=t-r_i/c_i$, $r_i=|\mathbf{p}_i'-\mathbf{p}|$, and $s=|\mathbf{p}-\mathbf{s}|$.

The specular reflection law implies that $dS_i'=dS_i$ for $i=1,2$. By differentiating Snell's law, it follows that $\cos\theta_1\,d\theta_1/c_1'=\cos\theta_2\,d\theta_2/c_2'$. For two-dimensional systems, the solid angles dS_i match with the emission angles $d\theta_i$ and so $\cos\theta_1\,dS_1/c_1'=\cos\theta_2\,dS_2/c_2'$. For three-dimensional systems, a direction in space is fully determined by two angles: θ the polar angle and β the angle lying in the interface plane. The infinitesimal solid angle is $dS=\sin\theta\,d\theta\,d\beta$. Multiplying the Snell's law and its derivative gives $\cos\theta_1\,dS_1/c_1'^2=\cos\theta_2\,dS_2/c_2'^2$. In any dimension $n=1$, 2, or 3, the relationship between the solid angles is $\cos\theta_1\,dS_1/c_1'^{n-1}=\cos\theta_2\,dS_2/c_2'^{n-1}$. Introducing the above Eqs. (28), (29), (30) into (26), (27)

$$\begin{aligned}\frac{\sigma_1(\mathbf{p},\mathbf{u}_1,t)}{\cos\theta_1}=\tau_{11}\Bigg[&\frac{\sigma_1(\mathbf{p}_1',\mathbf{u}_1',t_1')}{\cos\theta_1'}e^{-m_1 r_1}\\&+\int_{\mathbf{p}_1'\mathbf{p}}\rho_1(\mathbf{s},\mathbf{u}_1',t-s/c_1)e^{-m_1 s}\,ds\Bigg]\\&+\left(\frac{c_2'}{c_1'}\right)^{n-1}\tau_{21}\Bigg[\frac{\sigma_2(\mathbf{p}_2',\mathbf{u}_2',t_2')}{\cos\theta_2'}e^{-m_2 r_2}\\&+\int_{\mathbf{p}_2'\mathbf{p}}\rho_2(\mathbf{s},\mathbf{u}_2',t-s/c_2)e^{-m_2 s}\,ds\Bigg],\end{aligned} \tag{31}$$

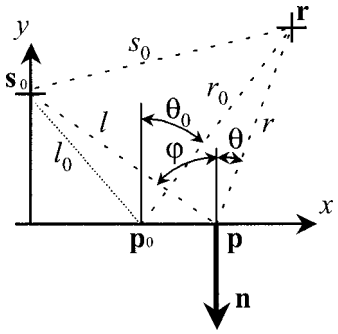

FIG. 4. A point source in a semi-infinite plane with a uniform reflectivity.

$$\frac{\sigma_2(\mathbf{p},\mathbf{u}_2,t)}{\cos\theta_2}=\left(\frac{c_1'}{c_2'}\right)^{n-1}\tau_{12}\left[\frac{\sigma_1(\mathbf{p}_1',\mathbf{u}_1',t_1')}{\cos\theta_1'}e^{-m_1r_1}+\int_{\mathbf{p}_1'\mathbf{p}}\rho_1(\mathbf{s},\mathbf{u}_1',t-s/c_1)e^{-m_1s}\,ds\right]+\tau_{22}\left[\frac{\sigma_2(\mathbf{p}_2',\mathbf{u}_2',t_2')}{\cos\theta_2'}e^{-m_2r_2}+\int_{\mathbf{p}_2'\mathbf{p}}\rho_2(\mathbf{s},\mathbf{u}_2',t-s/c_2)e^{-m_2s}\,ds\right]. \quad (32)$$

Thus, two functional equations are obtained for the unknown variables σ_1 and σ_2.

VI. IMAGE-SOURCE SOLUTION

The solution of Eq. (22) via the image-source technique is now presented. The calculations are based on the expression of the delta Dirac function in a polar coordinate system. Consider a half-plane where a single source $\mathbf{s}_0(0,h)$ acts as shown in Fig. 4. The source generates a time-varying injected power $P_{\text{inj}}(t)$. The boundary Γ, defined by $y=0$, has a uniform reflectivity $\tau=1-\alpha$. Let $\mathbf{p}(\nu,0)$ be any point on the boundary and θ any emission angle. Accounting for the nonexistence of the point $\mathbf{p}'$, Eq. (22) gives

$$\frac{\sigma(\nu,\theta,t)}{\cos\theta}=\tau\int_{\infty\mathbf{p}}\delta_{\mathbf{s}_0}(\mathbf{s})P_{\text{inj}}(t-s/c)e^{-ms}\,ds, \quad (33)$$

where $\infty\mathbf{p}$ is the semi-infinite incident line of direction $-\theta$, with an end point $\mathbf{p}$. As usual, $s=|\mathbf{p}-\mathbf{s}|$. For the polar coordinate system centered at $\mathbf{p}$, the delta Dirac function can be written as

$$\delta_{\mathbf{s}_0}(s,\theta)=\frac{\delta(s-l)}{s}\,\delta(\theta-\varphi), \quad (34)$$

where $l=|\mathbf{p}-\mathbf{s}_0|=(\nu^2+h^2)^{1/2}$ and φ is the incidence angle at $\mathbf{p}$ from $\mathbf{s}_0$. Then,

$$\sigma(\nu,\theta,t)=\tau P_{\text{inj}}(t-l/c)\cos\theta\frac{e^{-ml}}{l}\,\delta(\theta-\varphi). \quad (35)$$

The above equality fully determines the variable σ.

Let $\mathbf{r}(x,y)$ be any point within the domain Ω $(y>0)$ as shown in Fig. 4. Substituting into Eq. (35), Eq. (11) yields

$$W(\mathbf{r},t)=P_{\text{inj}}\left(t-\frac{s_0}{c}\right)\frac{e^{-ms_0}}{\gamma_0cs_0}+\tau\int_{-\infty}^{\infty}P_{\text{inj}}\left(t-\frac{l+r}{c}\right)\times\cos\theta\frac{e^{-ml}}{l}\,\delta(\theta-\varphi)\frac{e^{-mr}}{2\pi cr}\,d\nu,$$

where $s_0=|\mathbf{r}-\mathbf{s}_0|$, $r=|\mathbf{r}-\mathbf{p}|$.

It should be noted that

$$\int_a^b g(x)\,\delta[f(x)]dx=\int_{f(a)}^{f(b)}g\frac{\delta[f]}{df/dx}df=\sum_i\frac{g[x_i]}{|df/dx[x_i]|}, \quad (36)$$

where the sum is running over all zeros x_i of f for the interval $[a,b]$. The absolute value stems from $f(b)\leqslant 0\leqslant f(a)$ when $df/dx\leqslant 0$.

Let $\psi(\nu)=\theta-\varphi$. The equation $\psi(\nu)=0$ has a unique solution ν_0 as shown in Fig. 4, $\theta_0=\varphi_0$. Let $r_0=|\mathbf{p}_0-\mathbf{r}|$ and $l_0=|\mathbf{p}_0-\mathbf{s}_0|$. From Fig. 4, an explicit value of ψ can be found

$$\psi=\arctan\frac{\nu-x}{y}+\arctan\frac{\nu}{h}. \quad (37)$$

Hence,

$$\frac{d\psi}{d\nu}=\frac{1/y}{1+\left(\frac{\nu-x}{y}\right)^2}+\frac{1/h}{1+\left(\frac{\nu}{h}\right)^2}=\frac{\cos\theta}{r}+\frac{\cos\varphi}{l} \quad (38)$$

and

$$W(\mathbf{r},t)=P_{\text{inj}}\left(t-\frac{s_0}{c}\right)\frac{e^{-ms_0}}{\gamma_0cs_0}+\tau P_{\text{inj}}\left(t-\frac{l_0+r_0}{c}\right)\times\frac{e^{-ml_0}}{l_0}\frac{e^{-mr_0}}{2\pi cr_0}\frac{\cos\theta_0}{\frac{\cos\theta_0}{r_0}+\frac{\cos\varphi_0}{l_0}}. \quad (39)$$

After simplification

$$W(\mathbf{r},t)=P_{\text{inj}}\left(t-\frac{s_0}{c}\right)\frac{e^{-ms_0}}{2\pi cs_0}+\tau P_{\text{inj}}\left(t-\frac{s_1}{c}\right)\frac{e^{-ms_1}}{2\pi cs_1}, \quad (40)$$

where $s_1=l_0+r_0$. In a similar way, it can be found that

$$\mathbf{I}(\mathbf{r},t)=P_{\text{inj}}\left(t-\frac{s_0}{c}\right)\frac{e^{-ms_0}}{2\pi s_0}\mathbf{u}_{\mathbf{s}_0\mathbf{r}}+\tau P_{\text{inj}}\left(t-\frac{s_1}{c}\right)\frac{e^{-ms_1}}{2\pi s_1}\mathbf{u}_{\mathbf{p}_0\mathbf{r}}. \quad (41)$$

The fields W and $\mathbf{I}$ are the sum of a direct field emerging from the source $\mathbf{s}_0(0,h)$ and a diffracted field emerging from a virtual source $\mathbf{s}_1(0,-h)$. This result is also valid for one-dimensional and three-dimensional systems. The total contribution of the diffraction sources, the second integral in Eqs. (11) and (12), collapses to a single spherical wave, i.e., the second term in the right-hand side of Eqs. (40) and (41).

This example suggests that Eqs. (11), (12), and (22) can be solved with the image-source technique. This technique is

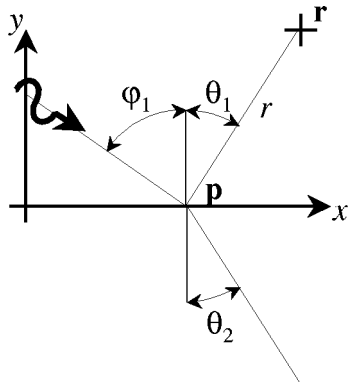

FIG. 5. Plane wave hitting an interface with uniform reflectivity.

efficient when the domain Ω has a simple form such as parallelepipeds or arbitrary polyhedra.[19] For convex domains, the image-sources $\mathbf{s}_i$ $i=1,2,\ldots$, are constructed by applying successive symmetries to the other sources with respect to the faces of the boundary. The number of symmetries k_i is referred to as the order of the image source. The fields within the domain Ω are constructed via the linear superposition of the fields created by actual and image sources

$$W(\mathbf{r},t)=\sum_{i=0}^{\infty} P_{\mathrm{inj}}(t-s_i/c)\,\tau^{k_i} G(\mathbf{s}_i,\mathbf{r}), \tag{42}$$

$$\mathbf{I}(\mathbf{r},t)=\sum_{i=0}^{\infty} P_{\mathrm{inj}}(t-s_i/c)\,\tau^{k_i} \mathbf{H}(\mathbf{s}_i,\mathbf{r}), \tag{43}$$

where $s_i=|\mathbf{r}-\mathbf{s}_i|$. The number of image sources may be finite or infinite. The solution of Eq. (22) is

$$\sigma(\mathbf{p},\theta,t)=-\gamma_0\sum_{i=1}^{\infty} P_{\mathrm{inj}}(t-s_i/c)\,\tau^{k_i}\mathbf{H}(\mathbf{s}_i,\mathbf{p})\cdot\mathbf{n}\,\delta(\theta-\theta_i), \tag{44}$$

with $s_i=|\mathbf{p}-\mathbf{s}_i|$, $\cos\theta_i=|\mathbf{n}\cdot\mathbf{u}_{\mathbf{s}_i\mathbf{p}}|$. Only image sources located behind point $\mathbf{p}$ contribute to an inward direction for σ. This solution provides an interpretation for the potential σ. The potential σ intercepts the power from all the image sources $\mathbf{s}_i$, re-emiting it regardless of the boundary.

VII. IRREVERSIBILITY AT THE INTERFACE

Consider an incident steady-state plane wave of magnitude A and direction $\mathbf{u}_1'$ hitting the interface between two semi-infinite undamped media with an angle of incidence φ_1, as shown in Fig. 5. The refracted angle is φ_2. For such a system, the diffraction source distributions σ_1, σ_2 do not depend upon the position and Eqs. (31), (32) take the form

$$\sigma_1(\theta_1)=A\tau_{11}\cos\theta_1\,\delta(\theta_1-\varphi_1), \tag{45}$$

$$\sigma_2(\theta_2)=A\frac{c_1'}{c_2'}\tau_{12}\cos\theta_2\,\delta(\theta_1-\varphi_1), \tag{46}$$

where θ_1 and θ_2 are related. Equation (11) leads to

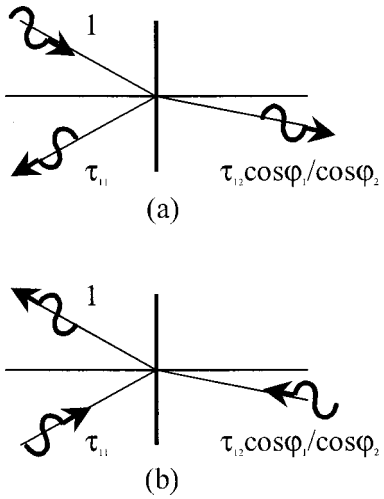

FIG. 6. Plane wave hitting an interface: (a) t-positive evolution, (b) t-negative evolution.

$$W_1(\mathbf{r})=\int_{-\pi/2}^{\pi/2}\frac{A}{2\pi c_1}\delta(\theta_1-\varphi_1)\,d\theta_1 + \int_{-\infty}^{\infty}\tau_{11}\frac{A}{2\pi c_1 r}\cos\theta_1\,\delta(\theta_1-\varphi_1)\,d\nu, \tag{47}$$

$$W_2(\mathbf{r})=\int_{-\infty}^{\infty}\tau_{12}\frac{A}{2\pi c_2 r}\frac{c_1'}{c_2'}\cos\theta_2\,\delta(\theta_1-\varphi_1)\,d\nu, \tag{48}$$

where $r=|\mathbf{r}-\mathbf{p}|$. With the changes of variable $d\nu=r\,d\theta_1/\cos\theta_1$ for the first equality and $d\nu=r\,d\theta_2/\cos\theta_2$ and $d\theta_2=c_2'\cos\theta_1\,d\theta_1/c_1'\cos\theta_2$ for the second equality

$$\begin{aligned} W_1(\mathbf{r}) &= \frac{A}{2\pi c_1}+\frac{A}{2\pi c_1}\int_{-\pi/2}^{\pi/2}\tau_{11}\frac{\cos\theta_1}{r} \\ &\quad\times\delta(\theta_1-\varphi_1)\frac{r}{\cos\theta_1}d\theta_1 \\ &= \frac{A}{2\pi c_1}[1+\tau_{11}], \end{aligned} \tag{49}$$

$$\begin{aligned} W_2(\mathbf{r}) &= \frac{A}{2\pi c_2}\int_{-\pi/2}^{\pi/2}\tau_{12}\frac{c_1'}{c_2'}\delta(\theta_1-\varphi_1)\,d\theta_2 \\ &= \frac{A}{2\pi c_2}\int\tau_{12}\frac{\cos\theta_1}{\cos\theta_2}\delta(\theta_1-\varphi_1)\,d\theta_1 \\ &= \frac{A}{2\pi c_2}\tau_{12}\frac{\cos\varphi_1}{\cos\varphi_2}. \end{aligned} \tag{50}$$

Corresponding results for energy flow vectors are

$$\mathbf{I}_1(\mathbf{r})=\frac{A}{2\pi}[\mathbf{u}_1'+\tau_{11}\mathbf{u}_1], \tag{51}$$

$$\mathbf{I}_2(\mathbf{r})=\frac{A}{2\pi}\tau_{12}\frac{\cos\varphi_1}{\cos\varphi_2}\mathbf{u}_2. \tag{52}$$

The fields in domain Ω_1 are the sum of an incident plane wave of magnitude A and a reflected plane wave of magnitude $A\tau_{11}$. The fields in domain Ω_2 are a transmitted plane wave of magnitude $A\tau_{12}\cos\varphi_1/\cos\varphi_2$. Figure 6(a) provides

a summary for the case $A=1$.

Now, suppose that time evolution is inverted, leading to the situation shown in Fig. 6(b). Consider two plane waves simultaneously hit the interface with magnitudes τ_{11} and $\tau_{12}\cos\varphi_1/\cos\varphi_2$. They both contribute to the reflective wave of unit magnitude and also to the nonexistent reflective wave which enters the domain Ω_2. The former is the sum of the reflective part τ_{11}^2 of the incident wave τ_{11} plus the transmitted part $\tau_{21}\cos\varphi_2/\cos\varphi_1\times\tau_{12}\cos\varphi_1/\cos\varphi_2$. Hence

$$\tau_{11}^2+\tau_{12}\tau_{21}=1. \tag{53}$$

Similarly

$$(\tau_{11}+\tau_{22})\tau_{12}=0. \tag{54}$$

As efficiencies are non-negative factors less than unity, the two conditions (53), (54) are only true for two trivial cases

$$\tau_{12}=0 \quad \text{and} \quad \tau_{11}=\tau_{22}=1, \tag{55}$$

$$\tau_{11}=\tau_{22}=0 \quad \text{and} \quad \tau_{12}=\tau_{21}=1. \tag{56}$$

The first case defines an impermeable interface. The second case implies that the interface is nonexistent. For all other cases, Eqs. (53) and (54) cannot be verified. Hence, the situation obtained by time reversing leads to self-contradiction. This lack of invariance under time reversal shows that the present theory is fundamentally irreversible. This irreversibility cannot be attributed to dissipative phenomena as the previous argument was applied to nondissipative media separated by a conservative interface. Hence, this irreversibility is distinguishable from the thermodynamic irreversibility which stems from the conversion of mechanical energy into heat. Appendix C shows, via an example, that the irreversibility under discussion originates from the uncorrelation assumption, which is not symmetric under time reversal. Neglecting the interference of ingoing waves is not equivalent to neglecting the interference of outgoing waves.

VIII. RAY-TRACING SOLUTION

Equation (22) may be solved in a general fashion, leading to an interpretation by means of a ray path. Let $\mathbf{p}_0$ be any regular point on the boundary. Equation (22) introduces a point $\mathbf{p}'$, also noted as $\mathbf{p}_1$ in this section, from which the incident energy originates. Writing Eq. (22) for point $\mathbf{p}_1$ leads to the definition of point $\mathbf{p}_2$. Noting $\mathbf{p}_1$, $\mathbf{p}_2$, $\mathbf{p}_3$, and so on, the successive points from which the energy is reflected, and $t_1,t_2,\ldots$, the successive times for the reflection where $t_k=t_{k-1}-r_k/c$ and $r_k=|\mathbf{p}_k-\mathbf{p}_{k-1}|$, Eq. (22) gives the following recursive relationship:

$$\frac{\sigma_k}{\cos\theta_k}=\tau_k\left[\frac{\sigma_{k+1}}{\cos\theta_{k+1}}e^{-mr_{k+1}}+\int_{\mathbf{p}_{k+1}\mathbf{p}_k}\rho(\mathbf{s},\mathbf{u}_{k+1},t_k-s/c)e^{-ms}\,ds\right], \tag{57}$$

where $s=|\mathbf{s}-\mathbf{p}_k|$. The subscript $k=0,1,\ldots$, defines the locations of point $\mathbf{p}_k$ and $\sigma_k=\sigma(\mathbf{p}_k,\mathbf{u}_k,t_k)$. Successive substitution of each equation into the previous leads to

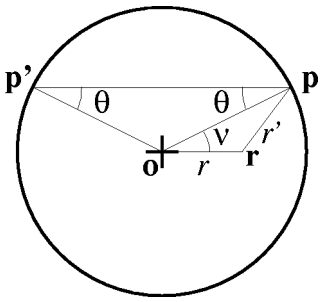

FIG. 7. Circular domain loaded at its center.

$$\frac{\sigma_0}{\cos\theta_0}=\sum_{k=0}^{n-1}\left(\prod_{i=0}^{k}\tau_i\right)\int_{\mathbf{p}_{k+1}\mathbf{p}_k}\rho(\mathbf{s},\mathbf{u}_{k+1},t-L(\mathbf{s})/c)\times e^{-mL(\mathbf{s})}\,dS+\mathcal{R}_n, \tag{58}$$

where $L(\mathbf{s})=s+r_k+\cdots+r_1$ is the total length from $\mathbf{s}$ to $\mathbf{p}_0$ and $\mathcal{R}_n=(\Pi_{i=0}^{n-1}\tau_i)\sigma_n e^{-mL(\mathbf{p}_n)}/\cos\theta_n$ and $L(\mathbf{p}_n)$ is the distance from $\mathbf{p}_n$ to $\mathbf{p}_0$ along the ray path. Assuming that the remaining term $\mathcal{R}_n$ tends to zero as n tends to infinite

$$\frac{\sigma(\mathbf{p}_0,\mathbf{u}_0,t)}{\cos\theta_0}=\sum_{k=0}^{\infty}\left(\prod_{i=0}^{k}\tau_i\right)\int_{\mathbf{p}_{k+1}\mathbf{p}_k}\rho(\mathbf{s},\mathbf{u}_{k+1},t-L(\mathbf{s})/c)e^{-mL(\mathbf{s})}\,ds. \tag{59}$$

Equation (59) may be considered the solution of Eq. (22) since it gives the diffraction sources σ solely in terms of the actual sources ρ.

The diffraction source σ at a point $\mathbf{p}_0$ in a direction $\mathbf{u}_0$ stems from the actual sources ρ located along the path $\mathbf{p}_0,\mathbf{p}_1,\ldots,\mathbf{p}_k\ldots$. Consider a source $\mathbf{s}$ located in the segment $\mathbf{p}_{k+1}\mathbf{p}_k$. This source contributes to the point $\mathbf{p}$ via the term $(\Pi_{i=0}^{k}\tau_i)\rho(\mathbf{s},\mathbf{u}_{k+1},t-L(\mathbf{s})/c)e^{-mL(\mathbf{s})}$. The reduction of the magnitude stems from the successive absorption phenomena due to the ray hitting the boundary $(\Pi_{i=0}^{k}\tau_i)$, and also the attenuation due to the propagation $(e^{-mL(\mathbf{s})})$.

This section highlights the analogy between the functional equations and the ray-tracing technique. More precisely, the exact solution of the functional equation may be found by determining the ray paths. In Appendix B, a simple example illustrates the difference between the ray-tracing technique and the functional equation method. Despite drastically different implementation, both methods produce similar results.

IX. CIRCULAR DOMAIN

The third example for which Eq. (22) is solved is a circular system of radius R. It is assumed that energy is supplied from a point load at the center $\mathbf{o}$. The reflectivity τ of the boundary is uniform.

Consider a point $\mathbf{p}$ located at the boundary with an emission angle θ. As a result of polar symmetry around $\mathbf{o}$, a field depends solely on the distance r from the center and not on the angular position. Hence, the potential $\sigma(\mathbf{p},\theta)$ reduces to $\sigma(\theta)$. Figure 7 shows the configuration of points $\mathbf{p}$, $\mathbf{p}'$, and $\mathbf{o}$. The triangle $\mathbf{pop}'$ is isosceles and hence angle θ' equals angle θ. In addition, $|\mathbf{p}-\mathbf{p}'|=2R\cos\theta$. Equation (22) yields

$$\frac{\sigma(\theta)}{\cos\theta}=\tau\frac{\sigma(\theta)}{\cos\theta}e^{-2mR\cos\theta}+\tau\int_{\mathbf{pp}'}A\,\delta_{\mathbf{o}}(\mathbf{s})e^{-ms}\,ds, \quad (60)$$

with $s=|\mathbf{s}-\mathbf{p}|$. Developing the delta Dirac function in the polar coordinates centered at $\mathbf{p}$, leads to

$$\sigma(\theta)=\frac{\tau\cos\theta}{1-\tau e^{-2mR\cos\theta}} \times\int_0^{2R\cos\theta}A\,\delta(\theta)\frac{\delta(s-R)}{s}e^{-ms}\,ds. \quad (61)$$

And

$$\sigma(\theta)=A\frac{e^{-mR}}{R}\frac{\tau}{1-\tau e^{-2mR}}\,\delta(\theta). \quad (62)$$

Consider a point $\mathbf{r}$ within domain Ω at a distance r from the center $\mathbf{o}$. The energy density is

$$W(r)=A\frac{e^{-mr}}{2\pi cr} +\int_0^{2\pi}A\frac{\tau e^{-mR}}{R(1-\tau e^{-2mR})}\,\delta(\theta)\frac{e^{-mr'}}{2\pi cr'}R\,d\nu, \quad (63)$$

where $r'=|\mathbf{p}-\mathbf{r}|$.

The first term on the right-hand side of Eq. (63) is the direct field, while the integral represents the diffracted field. As in Sec. VI, $\theta(\nu)=0$ must be solved. From Fig. 7, it is clear that $\theta(\nu)$ vanishes when $\nu=0$ and $\nu=\pi$. In addition, the triangle **rop** shows that $r\sin\nu=r'\sin\theta$. By differentiating with respect to ν

$$r\cos\nu=\frac{dr'}{d\nu}\sin\theta+r'\cos\theta\frac{d\theta}{d\nu}. \quad (64)$$

For $\nu=0$ and $\nu=\pi$

$$\nu=0\quad |\mathbf{p}_0-\mathbf{r}|=R-r\quad \frac{d\theta}{d\nu}_{/\nu=0}=\frac{r}{R-r}, \quad (65)$$

$$\nu=\pi\quad |\mathbf{p}_0-\mathbf{r}|=R+r\quad \frac{d\theta}{d\nu}_{/\nu=\pi}=\frac{-r}{R+r}. \quad (66)$$

Applying the equality (36)

$$W(r)=\frac{A}{2\pi c}\frac{e^{-mr}}{r}+\frac{A}{2\pi c}\frac{\tau e^{-mR}}{1-\tau e^{-2mR}} \times\left[\frac{e^{-m(R-r)}}{(R-r)\dfrac{r}{R-r}}+\frac{e^{-m(R+r)}}{(R+r)\dfrac{r}{R+r}}\right]. \quad (67)$$

And finally

$$W(r)=\frac{A}{2\pi c}\frac{1}{1-\tau e^{-2mR}}\frac{e^{-mr}}{r}+\frac{A}{2\pi c}\frac{\tau e^{-2mR}}{1-\tau e^{-2mR}}\frac{e^{mr}}{r}. \quad (68)$$

Similarly

$$I(r)=\frac{A}{2\pi}\frac{1}{1-\tau e^{-2mR}}\frac{e^{-mr}}{r}-\frac{A}{2\pi}\frac{\tau e^{-2mR}}{1-\tau e^{-2mR}}\frac{e^{mr}}{r}, \quad (69)$$

for the radial component of the energy flow. The orthoradial component vanishes.

The energy field is found to be the sum of a field emerging from the center together with a field directed towards the center. This result agrees with those obtained in Ref. 20, where a more direct approach was employed. The first field is a *propagating wave*, whereas the second is a *retropropagating wave*.

X. CONCLUSION

A mathematical formalism which extends the ''standard procedure'' or ''radiosity method'' when applied to specular reflection is proposed in this paper. Energy fields are constructed by a superposition of uncorrelated elementary waves.

The study of this formalism identifies several important features. First, the underlying equations may be solved via the image-source method and may be interpreted in terms of rays. The resulting solutions are similar to those of geometrical optics or acoustics when the phase of the ray is not considered. Second, this formalism is well-suited to the study of two media separated by an interface. Incident waves reflect according to the standard laws of reflection and refraction and the energy ratios are determined by the efficiencies. The situation is irreversible. The irreversibility is not due to dissipative phenomena, but is caused by the neglection of the interference between inward waves, which are asymmetric under time reversal. This is a typical example of where an approximation of a fundamentally reversible phenomenon leads to an apparent irreversibility.

The next stage of this study is the development of software, which is capable of solving of Eq. (22) for more complicated situations. This would provide an alternative to the standard ray-tracing softwares.

APPENDIX A

This Appendix determines whether the local power balance equation (13) holds for complete fields (11) and (12) and also gives the proof of Eqs. (15) and (16).

The left-hand side of Eq. (13) must be evaluated. Reversing the order of the derivative and integral

$$\begin{aligned}\mathrm{div}\cdot\mathbf{I}+mcW+\frac{\partial W}{\partial t}&=\int_\Omega \mathrm{grad}_{\mathbf{r}}\rho.\mathbf{H}+\frac{\partial\rho}{\partial t}G\,d\Omega_{\mathbf{s}}\\ &\quad+\int_\Omega\rho[\mathrm{div}_{\mathbf{r}}\cdot\mathbf{H}+mcG]\,d\Omega_{\mathbf{s}}\\ &\quad+\int_\Gamma \mathrm{grad}_{\mathbf{r}}\sigma\cdot\mathbf{H}+\frac{\partial\sigma}{\partial t}G\,d\Gamma_{\mathbf{p}}\\ &\quad+\int_\Gamma\sigma[\mathrm{div}_{\mathbf{r}}\cdot\mathbf{H}+mcG]\,d\Gamma_{\mathbf{p}}.\end{aligned} \quad (A1)$$

The similarity of the first and third integrals on the right-hand side of Eq. (A1) should be noted. The expression

$$\mathrm{grad}_{\mathbf{r}}\rho(\mathbf{s},\mathbf{u_{sr}},t-s/c)\cdot\mathbf{H}(\mathbf{s},\mathbf{r})+\frac{\partial}{\partial t}\rho(\mathbf{s},\mathbf{u_{sr}},t-s/c)G(\mathbf{s},\mathbf{r}), \tag{A2}$$

with $s=|\mathbf{s}-\mathbf{r}|$, must be evaluated. Consider polar coordinates centered at **s**. The first term of Eq. (A2) is the radial component of the gradient. The above expression therefore becomes

$$\frac{\partial}{\partial s}\rho(\mathbf{s},\mathbf{u_{sr}},t-s/c)cG+\frac{\partial}{\partial t}\rho(\mathbf{s},\mathbf{u_{sr}},t-s/c)G=0. \tag{A3}$$

The first and third integrals in Eq. (A1) vanish. Using the local power balance for steady-state elementary waves[8]

$$\mathrm{div}_{\mathbf{r}}\cdot\mathbf{H}+mcG=\delta_{\mathbf{s}}, \tag{A4}$$

it yields

$$\mathrm{div}\cdot\mathbf{I}+mcW+\frac{\partial W}{\partial t}=\int_{\Omega}\rho\,\delta_{\mathbf{s}}(\mathbf{r})d\Omega_{\mathbf{s}}+\int_{\Gamma}\sigma\delta_{\mathbf{p}}(\mathbf{r})d\Gamma_{\mathbf{p}}. \tag{A5}$$

The second integral vanishes as the point **r** is inside Ω. In order to evaluate the first integral, the Dirac function is used with polar coordinates centered at **r**

$$\delta_{\mathbf{r}}(\mathbf{s})=\frac{1}{\gamma_0}\frac{\delta(s)}{s}. \tag{A6}$$

Expanding the integral

$$\int_{\Omega}\rho\,\delta_{\mathbf{r}}(\mathbf{s})d\Omega_{\mathbf{s}}=\int_0^{\infty}\int_{S_{n-1}}\rho\frac{\delta(s)}{\gamma_0 s}s\,dS\,ds. \tag{A7}$$

Thus

$$\mathrm{div}\cdot\mathbf{I}+mcW+\frac{\partial W}{\partial t}=p_{\mathrm{inj}}, \tag{A8}$$

with

$$p_{\mathrm{inj}}=\int_{S_{n-1}}\rho(\mathbf{r},\mathbf{u},t)dS_{\mathbf{u}}, \tag{A9}$$

which is the expected result.

For the proof of Eqs. (15) and (16) for the fields at the boundary Γ, consider a regular point $\mathbf{p}\in\Gamma$ and the hemisphere HS_ϵ, which is centered at **p**, with radius ϵ and is outside Ω (Fig. 8). Γ_ϵ denotes the segment of Γ which is outside the hemisphere HS_ϵ. Ω_ϵ denotes Ω plus the hemisphere HS_ϵ. When $\epsilon\to 0$ the boundary layer σ of the warped boundary must tend to a regular boundary. Consider the radiative intensity $I(\mathbf{p},\mathbf{u},t)$ of the surface $d\Gamma$ in the direction **u**, which is defined as the power per unit solid angle divided by the surface normal to the ray $d\Gamma_n=d\Gamma\cos\theta$ [Fig. 8(a)]. According to this definition, the source $\sigma\,d\Gamma$ radiates the intensity $I=\sigma(\mathbf{p},\mathbf{u},t)/\gamma_0\cos\theta$ in the direction **u**. On the other hand, the source $\sigma\,d\Gamma_{\mathbf{q}}$, located at a distance ϵ, emanates the intensity $I_\epsilon=\sigma(\mathbf{q},\mathbf{u},t-\epsilon/c)e^{-m\epsilon}/\gamma_0$ [Fig. 8(b)]. Both boundaries are equivalent, i.e., radiate the same intensity, under the condition that $\lim_{\epsilon\to 0}\sigma(\mathbf{q},\mathbf{u},t-\epsilon/c)e^{-m\epsilon}=\sigma(\mathbf{p},\mathbf{u},t)/\cos\theta$.

Evaluating the expressions (11) and (12) for the fields W and **I**, at point **p** in the domain $\Gamma_\epsilon\cup HS_\epsilon$

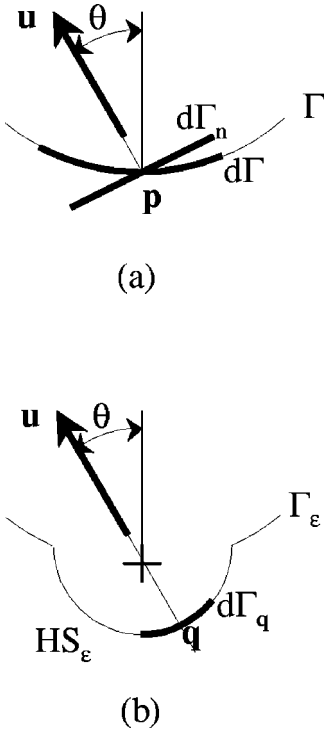

FIG. 8. Determination of the fields at the boundary: radiative intensity of the (a) regular boundary, (b) warped boundary.

$$W(\mathbf{p},t)=\int_{\Omega_\epsilon}\rho(\mathbf{s},\mathbf{u_{sp}},t-s/c)G(\mathbf{s},\mathbf{p})d\Omega_{\mathbf{s}}+\int_{\Gamma_\epsilon\cup HS_\epsilon}\sigma(\mathbf{q},\mathbf{u_{qp}},t-\epsilon/c)G(\mathbf{q},\mathbf{p})d\Gamma_{\mathbf{q}}, \tag{A10}$$

$$\mathbf{I}(\mathbf{p},t)=\int_{\Omega_\epsilon}\rho(\mathbf{s},\mathbf{u_{sp}},t-s/c)\mathbf{H}(\mathbf{s},\mathbf{p})d\Omega_{\mathbf{s}}+\int_{\Gamma_\epsilon\cup HS_\epsilon}\sigma(\mathbf{q},\mathbf{u_{qp}},t-\epsilon/c)\mathbf{H}(\mathbf{q},\mathbf{p})d\Gamma_{\mathbf{q}}, \tag{A11}$$

where $s=|\mathbf{s}-\mathbf{r}|$. When $\epsilon\to 0$, the first integral is regular and becomes $\lim_{\epsilon\to 0}\int_{\Omega_\epsilon}\rho G\,d\Omega=\int_\Omega\rho G\,d\Omega$. Separate the second integral in two terms gives $\int_{\Gamma_\epsilon}\sigma G\,d\Gamma+\int_{HS_\epsilon}\sigma G\,d\Gamma$. The first term tends to the principal value of Cauchy $\lim_{\epsilon\to 0}\int_{\Gamma_\epsilon}\sigma G\,d\Gamma=\int_\Gamma^{*}\sigma G\,d\Gamma$. For the second term, a change of variable is employed $d\Gamma_{\mathbf{q}}=\epsilon^{n-1}\,dS$

$$\int_{HS_\epsilon}\sigma G\,d\Gamma=\int_{HS}\sigma(\mathbf{q},\mathbf{u},t-\epsilon/c)\frac{e^{-m\epsilon}}{\gamma_0 c\,\epsilon^{n-1}}\epsilon^{n-1}\,dS_{\mathbf{u}}. \tag{A12}$$

Therefore, by virtue of the previous equivalence condition

$$\lim_{\epsilon\to 0}\int_{HS_\epsilon}\sigma G d\Gamma=\int_{HS}\frac{\sigma(\mathbf{p},\mathbf{u},t)}{\gamma_0 c\cos\theta}dS_{\mathbf{u}}. \tag{A13}$$

Equations (15), (16) for the fields on the boundary are hence proved.

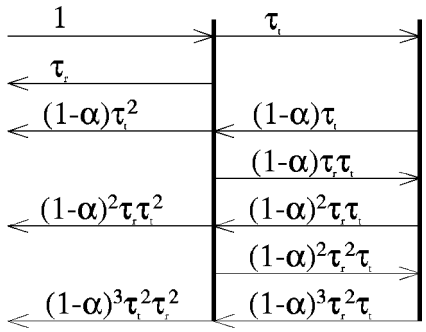

(a)

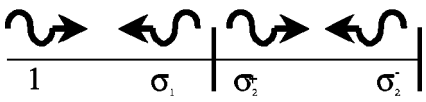

(b)

FIG. 9. Ray of unit magnitude hitting an interface: (a) ray-tracing solution; (b) solution via the use of Eqs. (22), (31), (32).

APPENDIX B

This Appendix is concerned with an example of a one-dimensional system, which illustrates the difference between the ray-tracing technique and the solving of the functional equations studied in this text.

Consider the one-dimensional system comprising two nondissipative media, one semi-infinite (on left), and the other finite (on right). For simplicity the interface is assumed to be reciprocal and the efficiencies are denoted τ_r and τ_t. α is the absorption factor of the right end. A right-traveling ray impinges on the interface.

The classical solution to this problem uses the ray-tracing technique.[13] When an incident ray of unit magnitude impinges upon the interface, it is separated into a reflected left-traveling ray in medium 1 of magnitude τ_r and a transmitted right-traveling ray in medium 2 of magnitude τ_t. The transmitted ray is partially reflected at the right end of the medium. The resulting reflected ray has the magnitude $(1-\alpha)\tau_t$. A new interface separation process occurs, giving two rays of magnitudes $(1-\alpha)\tau_t^2$ and $(1-\alpha)\tau_r\tau_t$. The latter is again reflected at the right end to produce a ray of magnitude $(1-\alpha)^2\tau_r\tau_t$, and so on. The ray paths and magnitudes are summarized in Fig. 9(a). The energies are obtained by summing the magnitudes of rays. The intensities are calculated by summing the algebraic magnitudes, taking into account the direction of propagation. Thus, the energies are

$$W_1 = 1+\tau_r+(1-\alpha)\tau_t^2\sum_{n=0}^{\infty}[(1-\alpha)\tau_r]^n = 1+\tau_r+\frac{(1-\alpha)\tau_t^2}{1-(1-\alpha)\tau_r}, \tag{B1}$$

$$W_2 = \tau_t[1+(1-\alpha)]\sum_{n=0}^{\infty}[(1-\alpha)\tau_r]^n = \frac{\tau_t(2-\alpha)}{1-(1-\alpha)\tau_r}. \tag{B2}$$

And the intensities

$$I_1 = c_1\left[1-\tau_r-(1-\alpha)\tau_t^2\sum_{n=0}^{\infty}[(1-\alpha)\tau_r]^n\right] = c_1\left[1-\tau_r-\frac{(1-\alpha)\tau_t^2}{1-(1-\alpha)\tau_r}\right], \tag{B3}$$

$$I_2 = c_2\left[\alpha\tau_t\sum_{n=0}^{\infty}[(1-\alpha)\tau_r]^n\right] = c_2\left[\frac{\tau_t\alpha}{1-(1-\alpha)\tau_r}\right]. \tag{B4}$$

An alternative means solving this problem is based on the formalism developed in this paper. The three boundary unknowns σ_1, σ_2^+, and σ_2^- [see Fig. 9(b)] are determined respectively by applying Eqs. (31), (32), and Eq. (22)

$$\begin{cases} \sigma_1 = \tau_r+\tau_t\sigma_2^- \\ \sigma_2^+ = \tau_t+\tau_r\sigma_2^- \\ \sigma_2^- = (1-\alpha)\sigma_2^+ \end{cases} \quad \text{then,} \quad \begin{cases} \sigma_1 = \tau_r+\dfrac{(1-\alpha)\tau_t^2}{1-(1-\alpha)\tau_r} \\ \sigma_2^+ = \dfrac{\tau_t}{1-(1-\alpha)\tau_r} \\ \sigma_2^- = \dfrac{\tau_t(1-\alpha)}{1-(1-\alpha)\tau_r}. \end{cases} \tag{B5}$$

The fields within the domains are given by Eqs. (11) and (12)

$$W_1 = 1+\sigma_1 = 1+\tau_r+\frac{(1-\alpha)\tau_t^2}{1-(1-\alpha)\tau_r}, \tag{B6}$$

$$W_2 = \sigma_2^+ + \sigma_2^- = \frac{\tau_t(2-\alpha)}{1-(1-\alpha)\tau_r}, \tag{B7}$$

$$I_1 = c_1[1-\sigma_1] = c_1\left[1-\tau_r-\frac{(1-\alpha)\tau_t^2}{1-(1-\alpha)\tau_r}\right], \tag{B8}$$

$$I_2 = c_2[\sigma_2^+ - \sigma_2^-] = c_2\left[\frac{\tau_t\alpha}{1-(1-\alpha)\tau_r}\right]. \tag{B9}$$

These results agree with those previously obtained.

Hence, the ray-tracing technique and the equations proposed in this paper may be considered as two alternative points of view for the same theory. The former is of a geometrical nature, whereas the latter is functional. The mathematical implementations are also quite different. The first method requires the calculation of a series, whereas the second method leads to a set of linear equations.

APPENDIX C

The noninvariance under time reversal means that neglecting the interference between waves entering to an interface is not equivalent to neglecting the interference between exiting waves. To check this assertion, consider two one-dimensional acoustical media with different velocities c_i and impedances Z_i $(i=1,2)$ jointed at $x=0$ as shown in Fig. 10.

In each medium the sound pressure may be viewed as the sum of a right-traveling wave $p_i^+(x)=a_i^+e^{j\omega(-x/c_i+t)}$

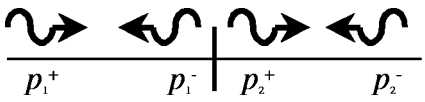

FIG. 10. Ingoing and outgoing waves hitting an interface between two acoustical one-dimensional media.

and a left-traveling wave $p_i^-(x)=a_i^- e^{j\omega(x/c_i+t)}$. At the interface, the conditions which ensure continuity of pressure and velocity are

$$\begin{aligned} &a_1^+ + a_1^- = a_2^+ + a_2^- \\ &(a_1^+ - a_1^-)/Z_1 = (a_2^+ - a_2^-)/Z_2. \end{aligned} \tag{C1}$$

Rearranging, to obtain the outgoing magnitudes in terms of entering magnitudes and conversely

$$\begin{cases} a_1^- = -\dfrac{Z_1 - Z_2}{Z_1 + Z_2} a_1^+ + \dfrac{2Z_1}{Z_1 + Z_2} a_2^- \\ a_2^+ = \dfrac{2Z_2}{Z_1 + Z_2} a_1^+ + \dfrac{Z_1 - Z_2}{Z_1 + Z_2} a_2^- \end{cases}$$

or (C2)

$$\begin{cases} a_1^+ = -\dfrac{Z_1 - Z_2}{Z_1 + Z_2} a_1^- + \dfrac{2Z_1}{Z_1 + Z_2} a_2^+ \\ a_2^- = \dfrac{2Z_2}{Z_1 + Z_2} a_1^- + \dfrac{Z_1 - Z_2}{Z_1 + Z_2} a_2^+. \end{cases}$$

The time-averaged energy flow supported by a plane wave is $P_i^{\pm} = |a_i^{\pm}|^2/2Z_i$. When the above systems are squared, the four powers $P_i^{\pm}$ appear with cross-product terms $|a_i a_j|$ which do not reduce to powers $P_i^{\pm}$. These terms are due to interference. As the waves are uncorrelated, these terms can be removed. Thus

$$\begin{pmatrix} P_1^- \\ P_2^+ \end{pmatrix}_i = \begin{pmatrix} \tau_r & \tau_t \\ \tau_t & \tau_r \end{pmatrix} \begin{pmatrix} P_1^+ \\ P_2^- \end{pmatrix}_i$$

or (C3)

$$\begin{pmatrix} P_1^+ \\ P_2^- \end{pmatrix}_o = \begin{pmatrix} \tau_r & \tau_t \\ \tau_t & \tau_r \end{pmatrix} \begin{pmatrix} P_1^- \\ P_2^+ \end{pmatrix}_o,$$

with $\tau_r = (Z_1 - Z_2)^2/(Z_1 + Z_2)^2$, $\tau_t = 4Z_1 Z_2/(Z_1 + Z_2)^2$, where the subscripts i and o denote, respectively, that ingoing and outgoing interferences have been neglected. Thus, the systems are shown not to be equivalent as the efficiency matrix is not unitary. As ingoing waves become outgoing waves, and vice versa when time evolution is reversed, the uncorrelation assumption is not invariant under time reversal.

[1] J. Barbry, "Techniques des images et des rayons (locaux vides)," Note Scientifique 51 INRS, France (1984).
[2] W. Joyce, "Sabine's reverberation time and ergodic auditoriums," J. Acoust. Soc. Am. **58**, 643–655 (1975).
[3] H. Kuttruff, "Simulierte nachhallkurven in rechteckräumen mit diffusem schallfeld," Acustica **25**, 333–342 (1971).
[4] R. Miles, "Sound field in a rectangular enclosure with diffusely reflecting boundaries," J. Sound Vib. **92**, 203–226 (1984).
[5] M. Carroll and C. Chien, "Decay of reverberent sound in a spherical enclosure," J. Acoust. Soc. Am. **62**, 1442–1446 (1977).
[6] H. Kuttruff, "Energetic sound propagation in rooms," Acta Acustica united with Acustica **83**, 622–628 (1997).
[7] M. F. Modest, *Radiative Heat Transfer* (McGraw-Hill, New York, 1993).
[8] A. Le Bot, "A vibroacoustic model for high frequency analysis," J. Sound Vib. **211**, 537–554 (1998).
[9] A. Le Bot, "Energy transfer for high frequencies in built-up structures," J. Sound Vib. **250**, 247–275 (2002).
[10] A. Le Bot and A. Bocquillet, "Comparison of an integral equation on energy and the ray-tracing technique for room acoustics," J. Acoust. Soc. Am. **108**, 1732–1740 (2000).
[11] H. Kuttruff, "Stationary propagation of sound energy in flat enclosures with partially diffuse surface reflection," Acta Acustica united with Acustica **86**, 1028–1033 (2000).
[12] H. Kuttruff, *Room Acoustics*, 3rd ed. (Elsevier Applied Science, London, 1991), see Eq. (1-15).
[13] J. Horner, and R. White, "Prediction of vibrational power transmission through jointed beams," Int. J. Mech. Sci. **32**, 215–223 (1990).
[14] W. Wöhle, T. Beckmann, and H. Schreckenbach, "Coupling loss factors for statistical energy analysis of sound transmission at rectangular slab joints. I," J. Sound Vib. **77**, 323–334 (1981).
[15] Y. Kravtsov and Y. Orlov, *Geometrical Optics of Inhomogeneous Media* (Springer, Berlin, 1990), see Sec. 2.5.
[16] R. Leung and R. Pinnington, "Wave propagation through right-angled joints with compliance-flexural incident wave," J. Sound Vib. **142**, 31–46 (1990), see Eq. (32).
[17] R. Langley, "A wave intensity technique for the analysis of high frequency vibrations," J. Sound Vib. **159**, 483–502 (1992), see Eq. (37).
[18] P. Morse and K. Ingard, *Theoritical Acoustics* (McGraw-Hill, New York, 1968), see Sec. 11.1.
[19] J. Borish, "Extension of the image model to arbitrary polyhedra," J. Acoust. Soc. Am. **75**, 1827–1836 (1984).
[20] A. Le Bot, "Geometric diffusion of vibrational energy and comparison with the vibrational conductivity approach," J. Sound Vib. **212**, 637–647 (1998).